

# Hierarchical Fault Diagnosis in Satellites Formation Flight

**Amitabh Barua, and K. Khorasani**

*Department of Electrical & Computer Engineering, Concordia University, Montreal, Quebec, H3G 1M8, Canada*

*a.barua@ece.concordia.ca*

*kash@ece.concordia.ca*

## ABSTRACT

Ground-support based satellite health monitoring and fault diagnosis practices involve around-the-clock limit-checking and trend analysis on large amount of telemetry data. They do not scale well for future multi-platform space missions due to the size of the telemetry data and an increasing need to make the long-duration missions cost-effective by limiting the operations team personnel. To utilize telemetry data efficiently, and to assist the less-experienced personnel in performing monitoring and diagnosis tasks, we have developed a hierarchical fault diagnosis methodology. The hierarchical decomposition is presented through a novel Bayesian Network (BN) whose structure is developed from the knowledge of component health state dependencies, and the parameters are obtained by a proposed methodology that utilizes both node diagnosis performance data and domain experts' beliefs. Our proposed model development procedure reduces the demand for expert's time in eliciting probabilities significantly, and our approach provides the ground personnel with an ability to perform diagnostic reasoning across a number of subsystems and components coherently. Due to the unavailability of real formation flight data, we demonstrate the effectiveness of our proposed methodology by using synthetic data of a leader-follower formation flight configuration. Although our proposed approach is developed from the satellite fault diagnosis perspective, it is generic and is targeted towards other types of cooperative fleet vehicle diagnosis problems.

## 1 INTRODUCTION

In the case of satellites that operate in near-Earth orbits, it has been possible to manage and operate these systems through additional design margins and extensive ground-based monitoring and control efforts.

This is an open-access article distributed under the terms of the Creative Commons Attribution 3.0 United States License, which permits unrestricted use, distribution, and reproduction in any medium, provided the original author and source are credited.

Fault diagnosis and health monitoring in the Earth orbiting single spacecraft missions are mostly accomplished by human operators at ground through around-the-clock limit-checking and trend analysis on large amount of telemetry data utilizing software tools. Current spacecraft diagnosis practices do not scale well for future multi-platform space missions due to the size of the telemetry data and an increasing need to make the long-duration missions cost-effective by limiting the operations team personnel. On the other hand, the effectiveness of spacecraft autonomy, which may be an ideal solution to this problem, is yet to be fully demonstrated. This is mainly constrained due to the existence of perceived risks for a fully autonomous system, which has necessitated that the expert human operators be involved in the spacecraft operations and diagnosis processes (Kurien and R-Moreno, 2008). Furthermore, in order to enhance the diagnostic performance and assist the less-experienced personnel in performing monitoring and diagnosis tasks at ground stations, there is a need for efficient utilization of the telemetry data (Iverson, 2008).

The concept of Integrated Vehicle Health Management (IVHM) is used to describe the automation of activities that are performed onboard as well as off-board by the ground support teams and maintenance personnel. Within an IVHM framework, offboard diagnosis of various components and subsystems are carried out by employing different types of reasoning algorithms such as Case-Based Reasoning (CBR), Rule-Based Reasoning (RBR), and Model-Based Reasoning (MBR). It is often the case that different design and development teams are involved in developing diagnostic algorithms for different components and subsystems. When these algorithms are employed independently and in isolation for diagnosing a specific component or subsystem, correlating faults that are identified at separate locations for assessing overall system health become nontrivial and difficult. Therefore, there is a need to provide the ground personnel with an ability to perform diagnostic reasoning coherently.

To address the above problems and requirements, in this paper we develop a systematic and transparent fault diagnosis methodology within the hierarchical fault diagnosis concepts and framework that we introduced in (Barua and Khorasani, 2007; 2008) for multi-platform space systems or satellites formation flight. We represent our proposed hierarchical decom-

position by a Component Dependency Model (CDM) using a novel Bayesian Network (BN) (Pearl, 1988; Jensen and Nielsen, 2007) structure. The structure of our CDM is determined from the knowledge of component health state dependencies. A methodology was developed for specifying the CDM parameters that quantify the health state dependencies and domain experts' beliefs. The present work is an extension of one of our earlier work (Barua and Khorasani, 2009) on spacecraft fault diagnosis.

The methodology that we have developed in this work for quantifying our CDM parameters is the result of and is being motivated by the inapplicability of the existing methods (for example, the ones in (Nikovski, 2000; Fenton *et al.*, 2007)) to our system as discussed in Section 2.2. Note that several belief or evidence propagation methods in BN are available in the literature (Pearl, 1988; Jensen and Nielsen, 2007), and the methods require that the BN parameters of the nodes be specified numerically. Our focus in the present paper is on BN-based fault diagnosis model development (structure and parameters) as opposed to the development of a belief propagation method.

The organization of the remaining parts of this paper is as follows: in Section 2, we develop a generic BN-based CDM that represents our proposed hierarchical framework for formation flight fault diagnosis. We discuss the purpose of our model, explain how the health states are defined at different nodes, develop procedure for specifying model parameters, and briefly discuss how evidences are generated at different nodes. In Section 3, we provide a description of the formation flight system simulation that we have utilized for synthetic data generation, and demonstrate our proposed fault diagnosis approach. In Section 4, we briefly discuss model accuracy and possible validation procedures of our model. Finally, conclusions are stated in Section 5.

## 2 BAYESIAN NETWORK MODEL FOR HIERARCHICAL FAULT DIAGNOSIS

Though the development of our proposed methodology is based on the health management of satellites formation flight, the methodology is generic enough to be applicable to other systems or a fleet of systems that require health monitoring decision support for the operators. Our proposed fault diagnosis strategy aims to perform diagnostic reasoning in complex systems such as a "formation flight system" by decomposing its complex structure hierarchically into simpler modules or components. The decomposition is driven by the need, from project management perspective, for supporting the development of the components/subsystems of the overall system by a number of teams and performing integration at the end.

First, we take into consideration that even if a fault is originated in a subsystem component, the fault is assumed to have different levels of manifestations in the hierarchy. In other words, for performing diagnosis at different levels, it is assumed that fault symptoms/manifestations are available. The definition of an "level  $l$  fault" (Barua and Khorasani, 2008) is formally stated as follows:

**Definition 2.1 (Level  $l$  Fault)** A fault occurring in a system that is hierarchically decomposed into  $L$  levels is said to be an "level  $l$  fault" ( $l = 1, 2, \dots, L$ ) and is denoted as fault  $f_k^l$  ( $k$ -th fault mode) if and only if its manifestations are only observable in the fault signatures that belong to level  $l$  and in higher levels for the fault severity level(s) under consideration.

Distinguishing faults at different levels based on the above definition would allow one to avoid cycles in our Bayesian Network (BN)-based fault diagnosis model which we have described in the subsequent sections. Furthermore, due to the presence of a functional hierarchy in the system, the components that are located at lower levels are commanded by the components that are located at higher levels. Consequently, in the case of a system level anomaly that leads to a situation in which a wrong command is sent to the subsystem component, the component would follow the wrong command, and the anomaly may not manifest in the subsystem component. The concept of level  $l$  fault allows one to identify fault manifestations systematically in the hierarchy.

### 2.1 Proposed Bayesian Network Model Structure and Node States

We represent our proposed hierarchical decomposition with a novel Bayesian network-based Component Dependency Model (CDM), as shown in Figure 1. The entire system under consideration is represented with a single node at the highest level and which consists of sub-components that are located at lower levels. We denote the  $p$ -th component at level  $l$  in the hierarchy as  $C_p^l$ . For example, if we consider a 4-level decomposition of a fleet of systems, for  $l = 1$ ,  $C_p^1$  would correspond to the  $p$ -th sensor or actuator (subsystem component) whereas for  $l = 4$ ,  $C_1^4$  would correspond to the "fleet". For the intermediate levels, i.e.,  $l = 2$  and  $l = 3$ , a component  $C_p^l$  would correspond to the  $p$ -th subsystem and system, respectively. Let  $L$  be the total number of levels in the hierarchy, and for any  $C_p^l$ , the set of components that are parents of  $C_p^l$  (as represented in Figure 1) is denote by  $pa(C_p^l)$ .

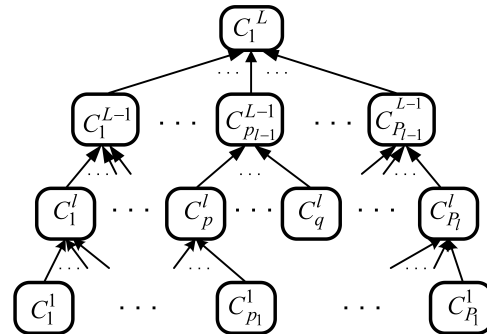


Figure 1: Bayesian network representation of our proposed hierarchical decomposition.

At this point, it is important to describe the *main objective* of our proposed hierarchical fault diagnosis and

health monitoring approach in detail. We intend to utilize our scheme as follows: when the faulty or healthy state of a node is observed by executing a diagnosis algorithm, the evidence (refer to Section 2.3) is introduced to our proposed CDM by instantiating that node. The evidence is propagated in the CDM by utilizing a standard propagation algorithm (such as the *junction tree algorithm*, *recursive conditioning algorithm*, etc.). In the nodes that have updated health states corresponding to the faulty states with high probabilities, diagnosis algorithms are executed to confirm the hypotheses. When a fault evidence is determined at some intermediate level in the hierarchy, the evidence is propagated downwards to identify the component in which the fault has originated from. On the other hand, the evidence is propagated upwards to identify components that are probably affected by the fault, and to determine if higher level specifications are still possible to be accomplished since the diagnosis algorithms at higher levels are usually based on certain rules that check the system (or, system of system) level specification.

It is possible to encounter situations where there is no identification of a faulty state at a higher level, whereas a low level fault is actually identified at a lower level. However, in such cases, it is worthwhile to propagate the evidence upwards in the hierarchy to identify the high level components that are possibly impacted by the identified fault. On the other hand, when the diagnosis at a higher level is accurate, it is worthwhile to propagate the evidence downwards in the hierarchy to identify the components where one should expect to observe fault manifestations even though fault identification cannot be performed at the current instant.

It should be noted that there are certain cost that is associated with performing fault diagnosis at each node in terms of data processing, algorithm development, validation and performance evaluation. Furthermore, in case of having a large number of components, it is natural from the users' resource considerations that the number of nodes that are to be actively/ round the clock monitored is as few as possible. Consequently, it is possible that diagnosis algorithms are not employed at some of the intermediate nodes but it is desired that the nodes be included in the diagnosis model to determine which subsystem or system a faulty node at lower levels belongs to. Such representation allows systematic fault cause identification. In subsequent paragraphs we will investigate a general case of an  $L$  level hierarchical decomposition.

**Node Health States:** The possible states of a given node in our proposed CDM represent the health states of the corresponding component. It should be clear, according to Definition 2.1 that the origin of a fault (level  $l$  fault) is at one of the nodes  $C_p^l$  (refer to Figure 1) for which  $pa(C_p^l) = \emptyset$ . If  $pa(C_p^l) \neq \emptyset$ , the states of the parent nodes have impact on the states of  $C_p^l$ , and the fault may manifest at  $C_p^l$  after originating from some other node at lower levels. Depending on whether a node  $C_p^l$  has parent nodes or not, we as-

sign its health state as follows: given a component  $C_p^l$  and its parents  $pa(C_p^l) = \{C_1^{l-1}, \dots, C_m^{l-1}, \dots, C_M^{l-1}\}$ , the possible health states  $X_p^l$  of  $C_p^l$  are represented as  $X_p^l = \{x_0, \dots, x_m, \dots, x_M\}$ ; where  $x_0$  corresponds to the state "healthy  $C_p^l$ " and  $x_m$  corresponds to the state "component  $C_m^{l-1}$  fault in  $C_p^l$ ". If  $pa(C_p^l) = \emptyset$ , the possible health states  $X_p^l$  of  $C_p^l$  are represented as  $X_p^l = \{x_0, \dots, x_k, \dots, x_K\}$ ; where  $x_k$  corresponds to the level  $l$  fault  $f_k^l$  that originates at  $C_p^l$ .

Note that it is possible to represent an anomaly in a node that corresponds to multiple simultaneous faults by a health state of the node. However, the diagnosis algorithm that is employed at that node must be capable of distinguishing among say, two single faults and their simultaneous occurrences. In such a case, from a fault identification perspective, the anomaly involving multiple faults can be treated as a "single fault" while generating a node performance evaluation matrix such as a confusion matrix (SAE, 2008). For sake of simplicity, in this paper we do not consider health states  $x_m \in X_p^l$  (or  $x_k \in X_p^l$ ) that correspond to multiple fault scenarios.

As mentioned above, node's states are observed by executing appropriate fault diagnosis algorithm at that node. Therefore, evidence should be introduced to network nodes when the states are identified by the diagnosis algorithms without ambiguity.

## 2.2 Determination of Model Parameters

Parameters of our proposed Bayesian network-based CDM are the conditional probabilities that are specified in the form of Conditional Probability Tables (CPT). It is well-known that the CPT that is specified at  $C_p^l$  has a number of parameters (conditional probabilities) that are exponential in the number of parents  $pa(C_p^l)$ ; i.e., one must specify  $P(X_p^l | pa(X_p^l))$  for each configuration of the parents. An overview of the methods that are commonly employed for probability elicitation from domain experts is available in (Renooij, 2000), and the limitations of eliciting probabilities exhaustively with domain experts are well-known. In our case, elicitation of CPTs from the domain expert opinions will be difficult because as the possible number of faults becomes large in the parent nodes of a given node, a number of parent configurations will become too specific for the expert to specify a distribution of the node's health state. Furthermore, it is not reasonable to assume that real data corresponding to different faults and all of their combinations are available. Generating synthetic data for combinations of fault occurrences will be cost prohibitive and challenging. Therefore, a requirement for parameter learning from data is likely to impose a significant barrier in model development and deployment.

Note that existing methods for generating CPTs are not useful in our case because of the following reasons: though noisy-OR (Jensen and Nielsen, 2007) is a well established method, it applies only to boolean nodes. The method available in (Nikovski, 2000) utilizes domain-dependent constraints that are not relevant to our problem. The method that is available

in (Fenton *et al.*, 2007) is also not applicable because it was developed for ranked nodes whose states are expressed on an ordinal scale which is mapped to a continuous, monotonically ordered, bounded numerical scale.

**Uncertainty Information:** Recall that our central problem at hand is to manage and utilize the health observations that are available from different sub-systems and components. In our proposed CDM, the health state of a given node is observed by employing appropriate fault diagnosis algorithms. Despite the fact that the algorithms are developed by different teams separately and are often proprietary to the teams, it is expected that the diagnosis algorithms that are employed at different nodes have their respective performance evaluation data, in the form of confusion matrices (SAE, 2008; Davison and Bird, 2008), available. It is possible to obtain the following conditional probabilities from the confusion matrix associated with a given node:  $P(X_p^l = x_k | I_p^l = x_n)$ ; where,  $N$  is the maximum possible value of  $k$  (and  $n$ ),  $k = 0, \dots, N$ ,  $n = 0, \dots, N$ , and  $I_p^l$  is the health state identification at the node. By utilizing these local conditional probabilities, one can derive the conditional probabilities that are necessary to specify  $P(X_p^l | pa(X_p^l))$ , and qualify the uncertainty in our proposed CDM as described in the subsequent paragraphs.

**Overview of the Proposed Procedure:** In (Laskey and Mahoney, 2000), it is argued that the care with which any given probability distribution needs to be elicited in a BN model depends strongly on the structure of the model and the queries that are intended to be processed. Our proposed procedure for CPT generation focuses on a set of initial distributions that are easily verifiable by a human expert. The idea is to construct a set of initial distributions from the information that is available in the confusion matrices, and provide a flexibility to a human expert for modification, if necessary. There may not be any need for modification if the expert agrees with the initial distributions. In this way, rather than asking the expert to provide a new distribution, we develop a procedure to construct distributions that the expert can modify, if necessary, according to his/her belief. These initial distributions mainly correspond to non-simultaneous sub-component (parent node) faults within a component (child node). Another rationale for providing the non-simultaneous sub-component faults significance and importance is due to the fact that most diagnosis algorithms are designed by incorporating this assumption.

**Initial Distributions:** Consider a generic segment of our proposed model as shown in Figure 2, where the child node  $C_p^l$  at level  $l$  has  $N$  parent nodes at level  $l-1$ ; i.e.,  $pa(C_p^l) = \{C_1^{l-1}, \dots, C_n^{l-1}, \dots, C_N^{l-1}\}$  and their corresponding number of health states are  $(m_1 + 1), \dots, (m_n + 1), \dots, (m_N + 1)$ . Consequently, the possible health states of  $C_p^l$  are  $X_p^l = \{x_0, \dots, x_n, \dots, x_N\}$

and the possible health states of the  $n$ -th parent node are  $X_n^{l-1} = \{x_i\}$ ;  $i = 0, 1, \dots, m_n$ . In other words, the possible number of parent configurations is  $\prod_{n=1}^N (m_n + 1)$ . Our objective is to determine a CPT that specifies  $P(X_p^l | X_1^{l-1}, \dots, X_N^{l-1})$ .

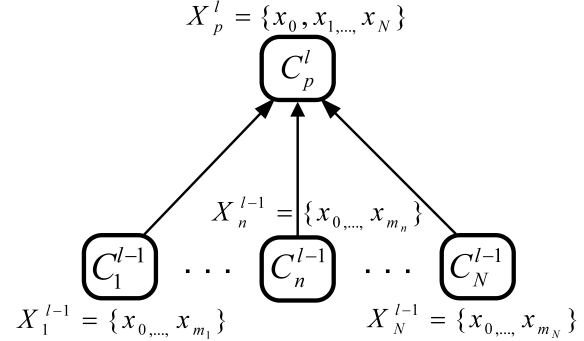


Figure 2: Health states of a child node at level  $l$  and its parent nodes at level  $l-1$ .

Let  $I_p^l$  denote the output of the health state identification algorithm that is employed at the node  $C_p^l$ . Hence, the possible outputs of  $I_p^l$  correspond to the possible node health states  $X_p^l$ ; i.e.,  $I_p^l = \{x_0, \dots, x_n, \dots, x_N\}$ . From the confusion matrix, it is possible to obtain the following information:  $P(X_p^l = x_k | I_p^l = x_n)$ ; where,  $k = 0, \dots, N$ , and  $n = 0, \dots, N$ . Similarly, at level  $l-1$ , the information available at the  $n$ -th sub-component of  $C_p^l$  are:  $P(X_n^{l-1} = x_k | I_p^{l-1} = x_i)$ ; where,  $k = 0, 1, \dots, m_n$  and  $i = 0, 1, \dots, m_n$ .

In order to determine the  $\prod_{n=1}^N (m_n + 1)$  belief or probability distributions  $P(X_p^l | X_1^{l-1}, \dots, X_N^{l-1})$  from the conditional probabilities above, first we focus on the distributions that correspond to single (non-simultaneous) component faults at level  $l-1$  and the one that corresponds to the healthy states of all the components at level  $l-1$ . Our objective is to determine  $N_\lambda + 1$  initial distributions over  $X_p^l$ , where  $N_\lambda = \sum_{j=1}^N m_j$ . Note that these distributions correspond to the parent configurations which can be verified relatively easily by a human expert. The  $N_\lambda$  initial distributions that correspond to the fault occurrences at level  $l-1$  are in the following general form

$$P(X_p^l | X_1^{l-1} = x_0, \dots, X_{n-1}^{l-1} = x_0, X_n^{l-1} = x_i, X_{n+1}^{l-1} = x_0, \dots, X_N^{l-1} = x_0) \quad (1)$$

where  $n = 1, \dots, N$  and  $i = 1, \dots, m_n$ . The remaining one initial distribution is as follows

$$P(X_p^l | X_1^{l-1} = x_0, \dots, X_n^{l-1} = x_0, \dots, X_N^{l-1} = x_0) \quad (2)$$

**Computation of Initial Distributions:** First, we note that there is a systematic pattern by which the health states at level  $l-1$  are mapped to the health states  $X_p^l$  at level  $l$  in our proposed CDM which is as follows:

**Observation 2.1 (Health State Mapping)**

The health states  $X_p^l$  of a component at level  $l$  and its sub-components at level  $l - 1$  are mapped as follows:

- $X_n^{l-1} = x_i; i = 1, \dots, m_n$  are mapped to the state  $X_p^l = x_n$  for a given component at level  $l - 1$ .
- $X_n^{l-1} = x_0; n = 1, \dots, N$  (non-faulty states of multiple components) are mapped to a single state  $X_p^l = x_0$ .

It is important to note that according to the way node health states are mapped in our modes, as stated in Observation 2.1,  $X_p^l = x_0$  is to be considered “true” only when all the parent nodes are healthy; i.e.,  $X_n^{l-1} = x_0; \forall n$ . It is now reasonable to state the following assumption.

**Assumption 2.1 (Independent Influences)** Faults or faulty states of the components at level  $l - 1$  influence the component health states at level  $l$  independently.

Assumption 2.1 is particularly valid if the target severity range (refer to Definition 2.1) is low and the components are monitored frequently enough so that the occurrences of faults in one component do not affect the fault identification in other components (Barua and Khorasani, 2008). Based on this independence assumption, the distribution in (1) is approximated as follows

$$\begin{aligned} &P(X_p^l | X_1^{l-1} = x_0, \dots, X_{n-1}^{l-1} = x_0, X_n^{l-1} = x_i, \\ &X_{n+1}^{l-1} = x_0, \dots, X_N^{l-1} = x_0) \\ &\approx \left( P(X_p^l = x_0 | X_{1,\dots,N}^{l-1} = x), \right. \\ &P(X_p^l = x_1 | X_n^{l-1} = x_i), \\ &\left. \dots, P(X_p^l = x_N | X_n^{l-1} = x_i) \right) \end{aligned} \quad (3)$$

where the first term is conditioned on the health states of all the parent sub-components at level  $l - 1$  with  $x \neq x_0$  for the  $n$ -th sub-component, and  $x = x_0$  otherwise. Since  $P(X_p^l) = 1$ , the distribution in Eq. (3) is subjected to the constraint

$$\sum_{j=1}^N P(X_p^l = x_j | X_n^{l-1} = x_i) = 1 \quad (4)$$

As indicated above, the conditional probabilities that are available from the confusion matrices at levels  $l$  and  $l - 1$  are local to the nodes at a given level. On the other hand, our problem is to quantify dependencies between levels  $l$  and  $l - 1$ . The difficulty is that due to different sensitivities of the diagnostic signals at the two levels there is no guarantee that whenever a fault is identified at level  $l - 1$  at a given instance, its manifestation at level  $l - 1$  is also identified at that instance as well or vice versa. One way to determine the dependencies is to conduct extensive experiments to observe the relative diagnostic performances of the nodes at the two levels for obtaining each CPT which is quite difficult, if not impossible. Alternatively, according to the way the health state mapping is set up in

our model, it is easy to see that whenever a faulty state  $X_n^{l-1} = x_i$  is identified at level  $l - 1$ , the component  $C_p^l$  becomes faulty (since  $C_n^{l-1}$  is a sub-component of  $C_p^l$ ) — whether the health state of  $C_p^l$  is identified as  $X_p^l = x_n$  or not. In the case where the fault is not identified at level  $l$ , the fault is latent in the sub-component  $C_n^{l-1}$  within  $C_p^l$ . Therefore, to practically overcome an unrealistic requirement for conducting extensive experiments, we propose to quantify dependencies by introducing the notion of *hierarchical health state agreement* as follows:

**Definition 2.2 (Hierarchical State Agreement)**

Given the health state mapping in Observation 2.1, and an identified fault that is manifested as  $X_p^l = x_n$ , ( $n \neq 0$ ) at level  $l$  and  $X_n^{l-1} = x_i$ , ( $i \neq 0$ ) at level  $l - 1$ , the health state identifications are in agreement if whenever  $I_p^l = x_n$  at level  $l$ ,  $I_n^{l-1} = x_i$ , at level  $l - 1$ .

Based on Definition 2.2, if  $I_p^l$  and  $I_n^{l-1}$  are known to be in agreement, given  $I_n^{l-1} = x_i$ , the probabilities of  $X_p^l$  and  $X_n^{l-1}$  are the same. We propose the following policy to quantify the degree of agreement by a *belief adjustment factor* that is denoted by  $h_{n,i}^{p,n}$  as follows

$$h_{n,i}^{p,n} = \begin{cases} a_{x_i}^{l-1} / a_{x_n}^l & \text{if } a_{x_i}^{l-1} < a_{x_n}^l \\ a_{x_n}^l / a_{x_i}^{l-1} & \text{if } a_{x_i}^{l-1} > a_{x_n}^l \end{cases} \quad (5)$$

where  $a_{x_n}^l$  is the accuracy with which the health state  $x_n$  is identified at level  $l$ . The notion of accuracy is computed by constructing a “one-versus-all” (Barua and Khorasani, 2008) decision matrix from the confusion matrix by following the procedure that is described in the next paragraph.

Let  $\mathbf{C}_{con}$  denote a  $(N + 1) \times (N + 1)$  confusion matrix associated with  $N + 1$  health states of a node at level  $l$  in which the actual and the identified health states are along the rows and the columns, respectively. To compute the accuracy in identifying the  $n$ -th state, a  $2 \times 2$  dimensional “one-versus-all” decision matrix  $\mathbf{C}_n$  is constructed as follows. Let  $c_{i,j}$  denote the element in the  $i$ -th row and the  $j$ -th column of  $\mathbf{C}_{con}$ , and  $c'_{i,j}$  denote the element in the  $i$ -th row and the  $j$ -th column of  $\mathbf{C}_n$ . The elements of the  $\mathbf{C}_n$  matrix are computed from  $c'_{2,2} = c_{n,n}$ ,  $c'_{2,1} = (\sum_{k=1}^N c_{n,k}) - c_{n,n}$ ,  $c'_{1,2} = (\sum_{k=1}^N c_{k,n}) - c_{n,n}$ , and  $c'_{1,1} = (\text{sum}(\mathbf{C}_{con}) - c'_{2,2} - c'_{2,1} - c'_{1,1})$ . The accuracy of identifying the  $n$ -th state is now defined as  $a_{x_n}^l = \text{trace}(\mathbf{C}_n) / \text{sum}(\mathbf{C}_n)$ .

Similar procedure is followed to determine  $a_{x_i}^{l-1}$ . The superscripts  $p, n$  in  $h_{n,i}^{p,n}$  correspond to the  $p$ -th component  $C_p^l$  and its  $n$ -th health state. The subscripts  $n, i$  correspond to the  $n$ -th sub-component of  $C_p^l$  and its  $i$ -th health state. It is important to note that the belief adjustment factor provides one’s degree of belief (in terms of probabilities) about the health states that should be decreased when the level  $l$  is changed. Therefore, if the probability of  $X_n^{l-1}$  is known given certain condition  $I$ , to find the probability of  $X_p^l$  given

the same condition  $I$ ,  $P(X_n^{l-1}|I)$  should be multiplied by the belief adjustment factor. We consider  $(1 - h_{n,i}^{p,n})$  to be a representative of the degree of disagreement.

It is not unusual that, in most cases, a diagnosis algorithm that is employed at a specific module or component meets the user specified accuracy (say,  $\gamma_{spec}$ ) in identifying the component health states by using the test data. For example, in (SAE, 2008), the acceptance criteria for fault isolation/identification given a detection is recommended as  $\gamma = 0.95$  in a major component; i.e., the deployed fault identification algorithms should be capable of identifying 95% of faults that are detected by the fault detection mechanism. Consequently,  $\gamma_{spec} \leq a_{x_n}^l \leq 1$ ,  $\gamma_{spec} \leq a_{x_i}^{l-1} \leq 1$ , and it follows that  $0 < h_{n,i}^{p,n} \leq 1$ ; where  $h_{n,i}^{p,n} = 1$  represents the highest degree of hierarchical agreement.

Note that at any two consecutive levels it is possible to have low accuracies but high belief adjustment factor. Furthermore, it is important to point out that the above policy is not precise, since according to Observation 2.1,  $a_{x_n}^l$  does not entirely correspond to a single faulty state  $X_n^{l-1} = x_i$ , ( $i \neq 0$ ). However, it should be clear that with the accuracy  $\gamma_{spec} \leq a_{x_i}^{l-1} \leq 1$  in identifying  $X_n^{l-1} = x_i$ ,  $i = 1, \dots, m_n$ , the policy is expected to be well-behaved.

Next, we determine the probability values corresponding to the approximated distribution in (3) which are categorized into the following three cases:

**Case 1:** Computation of  $P(X_p^l = x_k | X_n^{l-1} = x_i)$  for  $k = n$

The probability  $P(X_p^l)$  is conditioned on a faulty state which is identified by observing the output of  $I_n^{l-1}$ . Therefore, assuming a hierarchical health state agreement (Definition 2.2) with the belief adjustment factor  $h_{n,i}^{p,n}$ , we propose the following:

$$\begin{aligned} & P(X_p^l = x_n | X_n^{l-1} = x_i) \\ & \approx P(X_p^l = x_n | I_n^{l-1} = x_i) \\ & = h_{n,i}^{p,n} \left( P(X_n^{l-1} = x_i | I_n^{l-1} = x_i) \right. \\ & \quad \left. + \sum_{j \neq i, j=1}^{m_n} P(X_n^{l-1} = x_j | I_n^{l-1} = x_i) \right) \end{aligned} \quad (6)$$

Note that the last term in equation (6) is necessary since eventhough a fault is misclassified as another fault in a component at level  $l - 1$ , the health state of the child component remains the same (faulty) because all faulty states of a particular parent are mapped to a single non-faulty state of the child node (refer to Observation 2.1).

**Case 2:** Computation of  $P(X_p^l = x_k | X_{1,\dots,N}^{l-1} = x)$  for  $k = 0$

The probability  $P(X_p^l = x_0 | X_n^{l-1} = x_i)$  is the probability that level  $l$  is at a healthy state given that it's  $n$ -th sub-component at level  $l - 1$  is at a faulty state  $x_i$ . Since this is a case of disagreement between the two

levels, we use the belief adjustment factor  $(1 - h_{n,i}^{p,n})$  in our following computations. Furthermore, since the state  $X_p^l = x_0$  is dependent on all the parent sub-components (Observation 2.1), we need to take into account the probabilities that are related to all the sub-components' healthy state as follows

$$\begin{aligned} & P(X_p^l = x_0 | X_{1,\dots,N}^{l-1} = x) \\ & \approx P(X_p^l = x_0 | I_n^{l-1} = x_i) \\ & \quad \prod_{j \neq n, j=1}^N P(X_p^l = x_0 | I_j^{l-1} = x_0) \\ & = (1 - h_{n,i}^{p,n}) P(X_n^{l-1} = x_0 | I_n^{l-1} = x_i) \\ & \quad \prod_{j \neq n, j=1}^N h_{j,0}^{p,0} P(X_j^{l-1} = x_0 | I_j^{l-1} = x_0) \end{aligned} \quad (7)$$

**Case 3:** Computation of  $P(X_p^l = x_k | X_n^{l-1} = x_i)$  for  $k \neq 0$  and  $k \neq n$

As in Case 2 above, this is a case of disagreement as well. However, in this case since  $k \neq 0$  and  $k \neq n$ , when the level  $l$  is at the state  $x_k$  there is no dependency that is represented in our dependency model (Observation 2.1) through which  $x_k$  can be related to the health state of the  $n$ -th sub-component at level  $l - 1$ . Therefore, the set of probabilities  $P(X_p^l = x_k | X_n^{l-1} = x_i)$ ,  $k = 1, \dots, N$  ( $k \neq 0$  and  $k \neq n$ ) represent uncertainties that are related to un-modeled dependencies. Given that the distribution in (3) has to satisfy the constraint in (4), we propose to distribute beliefs equally among the set as follows

$$\begin{aligned} & P(X_p^l = x_k | X_n^{l-1} = x_i) \\ & = \frac{1}{N-1} \left( 1 - P(X_p^l = x_n | X_n^{l-1} = x_i) \right. \\ & \quad \left. - P(X_p^l = x_0 | X_{1,\dots,N}^{l-1} = x) \right) \end{aligned} \quad (8)$$

where  $k \neq 0$  and  $k \neq n$ . The procedure for computing  $P(X_p^l = x_n | X_n^{l-1} = x_i)$  and  $P(X_p^l = x_0 | X_{1,\dots,N}^{l-1} = x)$  are described in Case 1 and Case 2, respectively.

Next, in order to determine the distribution in (2) we observe that  $X_p^l = x_0$  only when **all** the parent sub-components are healthy. To avoid any ambiguity, we denote the distribution in (2) by  $P(X_p^l | X_{1,\dots,N}^{l-1} = x_0)$ . By Assumption 2.1, we propose to compute the distribution as follows

$$\begin{aligned} & P(X_p^l = x_0 | X_{1,\dots,N}^{l-1} = x_0) \\ & = 1 - P(X_p^l = \bar{x}_0 | X_{1,\dots,N}^{l-1} = x_0) \\ & = 1 - \prod_{j=1}^N (1 - h_{j,0}^{p,0}) P(X_j^{l-1} = \bar{x}_0 | I_j^{l-1} = x_0) \end{aligned} \quad (9)$$

where  $\bar{x}_0$  corresponds to the set  $\{X_p^l\} \setminus x_0$  or  $\{X_n^{l-1}\} \setminus x_0$  depending on the level in the hierarchy.

The remaining probabilities in the distribution in (2), i.e.,  $P(X_p^l = x_k | X_{1,\dots,N}^{l-1} = x_0)$  where  $k = 1, \dots, N$ , represent un-modeled dependencies since according to Observation 2.1, non-faulty states at level  $l-1$  are not mapped to faulty states at level  $l$ . In such a situation, as in Case 3 above, we propose to distribute beliefs equally among the set as follows

$$\begin{aligned} P(X_p^l = x_k | X_{1,\dots,N}^{l-1} = x_0) \\ = \frac{1}{N} \left( 1 - P(X_p^l = x_0 | X_{1,\dots,N}^{l-1} = x_0) \right) \end{aligned} \quad (10)$$

**Computation of Initial Distributions When Nodes Are Not Actively Monitored:** As mentioned in Section 2.1, it may be the case that some nodes in our proposed CDM are not monitored actively. Consequently, fault diagnosis algorithms are not deployed in those nodes. However, since our proposed node health state assignments follow a systematic pattern (refer to Section 2.1 and Observation 2.1), it is easy to observe that the distributions in (1) or (3) are expected to be maximum at  $X_p^l = x_n$  assuming that the accuracy of the diagnosis algorithm satisfies the user specification  $\gamma_{spaec}$ . Similarly, the distribution in (2) is expected to be maximum at  $X_p^l = x_0$ . Therefore, the initial distributions are specified such that the following conditions are satisfied:

$$\begin{aligned} \operatorname{argmax}_{x_n \in X_p^l} P(X_p^l | X_{1,\dots,N}^{l-1}) \\ = \begin{cases} x_n & \text{for the distributions in (1)} \\ x_0 & \text{for the distribution in (2)} \end{cases} \end{aligned} \quad (11)$$

In order to satisfy the above conditions, in the case of missing information first we assume a near-maximum hierarchical agreement and set  $h_{n,i}^{p,n}$  (in Eqs. (6) and (7)), and  $h_{j,0}^{p,0}$  (in Eqs. (7) and (9)) a value that is close to 1. Next, we assume ‘‘ideal’’ probabilities by setting  $P(X_n^{l-1} = x_i | I_n^{l-1} = x_i) = \beta_{11}$  (in Eq. (6)),  $P(X_n^{l-1} = x_0 | I_n^{l-1} = x_i) = \beta_{01}$  and  $P(X_j^{l-1} = x_0 | I_j^{l-1} = x_0) = \beta_{00}$  (in Eq. (7)), and  $P(X_j^{l-1} = \bar{x}_0 | I_j^{l-1} = x_0) = (1 - \beta_{00})$  (in Eq. (9)); where  $\beta_{11} \approx \gamma_{spec}$ ,  $\beta_{01} \approx (1 - \gamma_{spec})$ ,  $\beta_{00} \approx \gamma_{spec}$ , and  $\gamma_{spec}$  is the desired (design specification) probability of the correct health state given an identification in the parent nodes if suitable diagnosis algorithms were employed.

Finally, in the case of a component  $C_p^{l-1}$  that does not have a confusion matrix available, but has a similar component  $C_q^{l-1}$  with the same health states (for example, the reaction wheel actuators in a three-axis active attitude control subsystem) and a common child node  $C_p^l$ , the confusion matrix of  $C_p^{l-1}$  may be considered to be the same as that associated with  $C_q^{l-1}$  in order to specify the distributions in the CPT at the child node  $C_p^l$ . For such a set of similar components, it is also possible to construct a common confusion matrix by including data from the components.

**Computation of the Remaining Distributions:** Once the initial distributions are determined, we propose

to compute the remaining distributions by using a weighted-sum of the initial distributions, as in (1) and (2), as follows:

$$P(X_p^l | X_{1,\dots,N}^{l-1}) = \sum_{j=1}^{N_\lambda+1} w_j P_j(X_p^l | X_{1,\dots,N}^{l-1}) \quad (12)$$

where  $P(X_p^l | X_{1,\dots,N}^{l-1})$  represents  $P(X_p^l | X_1^{l-1}, X_2^{l-1}, \dots, X_N^{l-1})$ ,  $P_j$  is an initial distribution,  $w_j \in W$ , and  $W$  is an  $(N_\lambda + 1)$  dimensional weight vector that is subjected to the constraint  $\sum_{j=1}^{N_\lambda+1} w_j = 1$ . It is suggested that the human experts are provided with the initial distributions and are asked to decide the weights  $w_j$  based on their judgements. Therefore, given the initial distributions, our proposed procedure would require that the number of weight parameters  $w_j$  that grows linearly with the total number of parent nodes’ health states.

It is worthwhile to note that as pointed out in (Fenton *et al.*, 2007), it is easy for the human experts to express their opinions in terms of such weight assignments. Therefore, eventhough our procedure is simple, it is consistent with how human experts develop their beliefs by starting from some ‘‘anchor’’ values and adjusting them to specify probabilities (*adjustment and anchoring* heuristics) (Kahneman *et al.*, 1982). Alternatively, one may choose to develop a weight assignment policy that is based on prior probabilities of the faults in the initial distributions under consideration. However, in order to minimize biases toward certain types of faults that are frequently identified, the policy should include other considerations such as component operating hours since some faults may develop only toward the end of life of the component whereas others may develop at early stages. Development of such a policy is beyond the scope of this work and has been left as part of our future work.

### 2.3 Node Health State Identification and Evidence Generation

As mentioned in Section 2.2, component/node health states are identified by employing appropriate/available fault diagnosis algorithms in our CDM nodes. We introduce evidences of health states at different nodes of our proposed CDM. We obtain such evidences by utilizing fuzzy Rule-Based Reasoning (RBR) (Barua and Khorasani, 2008) at various nodes of our proposed CDM. Once the health state  $x_k \in X_p^l$  of  $C_p^l$  is identified by employing RBR (or any other reasoning algorithm that is employed at  $C_p^l$ ) at a given instance, an evidence over the  $K$  possible states of  $C_p^l$  is generated as follows:  $e_p^l = \{x_0 = 0, \dots, x_i = 1, \dots, x_K = 0\}$ , and introduced to the  $C_p^l$  node of our proposed CDM.

### 3 FAULT DIAGNOSIS RESULTS FOR SATELLITES FORMATION FLIGHT CASE STUDY

In this section, we demonstrate the fault diagnosis methodology that was presented in Section 2 by utilizing synthetic data. Note that utilization of synthetic

formation flying system data has been necessary due to the unavailability of actual telemetry data from multi-platform space missions which are still mostly in planning and design stages. We first provide a brief description of our data generation model before presenting the fault diagnosis results.

In a leader-follower formation flight, since the leader acts as a reference point, and the formation flying mission is subjected to a single-point failure of the leader satellite, we propose to reduce the health management workload for only the follower satellites by utilizing our proposed BN-based CDM. We assume that the components of the leader are monitored and diagnosed frequent enough to ensure that the leader is fault free before carrying out the monitoring and diagnosis of the follower satellites.

### 3.1 Formation Flying Mission and System Description

For synthetic fault data generation, first we have implemented and simulated high fidelity attitude control and power subsystems models of a planetary environment orbit (PEO) formation flying system with 5 identical small satellites (150 kg) in a leader-follower (LF) configuration as shown in Figure 3. An arrow from Sat- $j$  to Sat- $i$  indicates that attitude measurements of Sat- $i$  are available with respect to Sat- $j$ . A Sun-synchronous Lower Earth Orbit (LEO) with 550 km altitude (orbital period: 95 min (approx.)) was selected as the leader's Keplerian orbit. Followers are assumed to follow fuel-optimal trajectories around the leader (Hill, 1878; Vadali *et al.*, 2002). A detailed description of the two subsystems namely, the attitude control subsystem (ACS) and the electrical power subsystem (EPS) that we have implemented for generating the synthetic data to demonstrate and illustrate our fault diagnosis approach is available in (Barua and Khorasani, 2009).

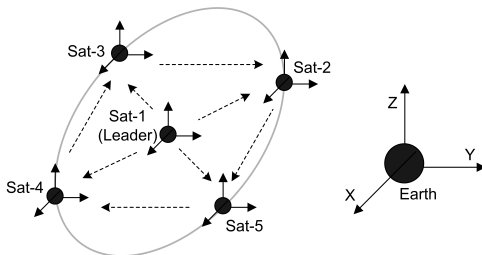


Figure 3: Formation flight of five satellites.

For synthetic data generation, in our ACS model, we have incorporated a high fidelity mathematical model of the *Ithaco Type-A* reaction wheel (RW) that is available in (Bialke, 1998). The model consists of detailed relationships for representing motor driver/torque control mechanism, motor disturbances such as cogging and ripple torques, Coulomb and viscous frictions, torque noise that results due to lubricant dynamics, the “EMF torque limiting” phenomenon at high speeds, safety mechanism for limiting speed, and torque bias discontinuity. We have also incorporated a simplified satellite electrical power subsystem (EPS) model, with our ACS model for each satellite. We have

modified the EPS model (Jiang *et al.*, 2003b), which is available in (USC-VTB-Team, 2009) and is developed in the virtual test bed (VTB) environment (Jiang *et al.*, 2003b; 2003a), to incorporate fault injection capabilities and to ensure the supply of desired bus voltage to the ACS reaction wheels.

It is important to mention that in our numerical simulations of the ACS, we have input the pre-generated EPS bus voltage data that corresponds to the orbital characteristics (altitude, inclination, eclipse period, etc.) of the satellites. Therefore, the interaction between the ACS and EPS is of the leader-follower type in the sense that any fault in the EPS may manifest in the ACS but the converse is not true. Such simulation setup is justified by the fact that the target ACS fault severities do not lead to excessively large deviations in the satellite attitude that may significantly affect the Sun pointing of the solar arrays, and hence the performance of the EPS.

**Fault Models** (refer to Figure 4): Within the ACS, two types of intermittent faults are considered and are injected at the subsystem component (reaction wheel) level: (a) friction fault (increase in the viscous friction), and (b) reaction wheel motor current fault (decrease in the motor gain). Within the EPS, two types of faults are considered at the subsystem level: (a) intermittent bus voltage drop due to the voltage regulator malfunctioning, and (b) intermittent bus voltage drop due to the anomaly in the battery.

Each fault is injected with 3 (three) severity levels: gradually increasing from the lowest to the maximum severity and then gradually decreasing before a complete fault removal. Note that the faults considered are *intermittent* and *non-abrupt* in nature. Although we are considering component level faults within the ACS, the faults corresponding to the EPS are considered at the subsystem level due to the lack of detailed models of the EPS components within the EPS. Consequently, the EPS fault diagnosis is performed only up to the subsystem level.

### 3.2 Implementation of Our Proposed Model and Fault Diagnosis Results

We have implemented a 4-level Bayesian network-based Component Dependency Model (CDM) for the formation flight of 5 satellites that was described above (refer to Figure 3). Towards this end, we have used the open source BN tool that is available from (UCLA, 2009). We have used the well-known *recursive conditioning* algorithm (Jensen and Nielsen, 2007) for belief propagation and updating. Figure 4 shows the implemented CDM where “Sat-1” ... “Sat-5” represent the five satellites in the formation, and “RW-X”, “RW-Y”, and “RW-Z” represent the reaction wheels (RW) in the X, Y, and Z directions, respectively.

First, we assign the states of the components  $C_p^l$  with  $pa(C_p^l) = \emptyset$  by following the procedure that was specified in Section 2. Each of the 15 RWs, denoted as  $C_i^1$ ; where  $i = 1, \dots, 15$  at level 1 (identified as the “subsystem component level”) is assigned the following three health states:  $X_i^1 = \{Healthy, friction\ fault, current\ fault\}$  (the fault models were discussed above). Each of the 5 electrical

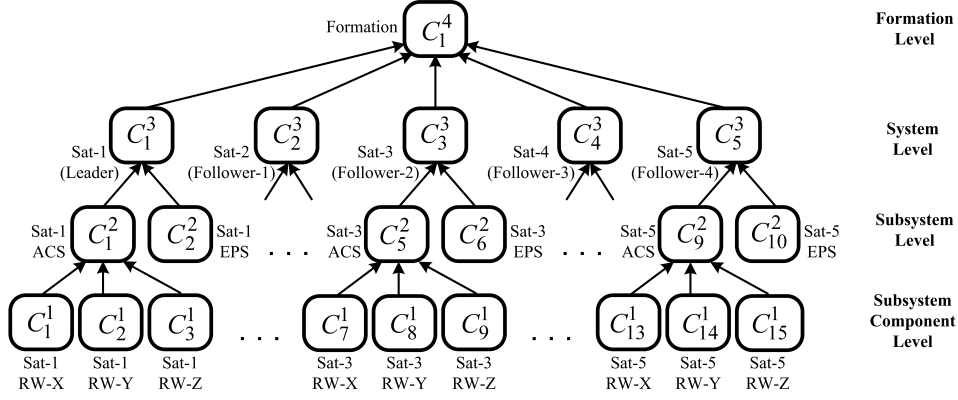


Figure 4: A 4-level Bayesian network-based component dependency model (CDM) for hierarchical fault diagnosis.

power subsystem (EPS) nodes, denoted as  $C_i^2$ ; where  $i = 2, 4, 6, 8, 10$  at level 2 (identified as the “subsystem level”) is assigned the following two health states:  $X_i^2 = \{Healthy, regulator\ fault, battery\ fault\}$  (the fault models were discussed above). We assume that at the beginning of the formation operation, the system is healthy and assign prior probabilities  $P(X_i^1) = \{0.9, 0.05, 0.05\}$ ; where  $i = 1, \dots, 15$ , and  $P(X_i^2) = \{0.9, 0.05, 0.05\}$ ; where  $i = 2, 4, 6, 8, 10$ , that represent the above assumption.

We assign the states of the components with  $pa(C_p^l) \neq \emptyset$  by following the procedure that was specified in Section 2. Each of the 5 attitude control subsystems (ACS) nodes, denoted as  $C_i^2$ ; where  $i = 1, 3, 5, 7, 9$  at level 2 is assigned the following four health states:  $X_i^2 = \{Healthy, RW.X\ fault, RW.Y\ fault, RW.Z\ fault\}$ . Each of the system level (level 3) nodes or satellites is assigned the following three health states:  $X_i^3 = \{Healthy, ACS\ fault, EPS\ fault\}$ . In the case of the formation component ( $C_1^4$ ), note that  $|pa(C_1^4)| = 5$  and each parent has 3 states which would lead to a large ( $3^5$ ) number of parent configurations. Consequently, first we have implemented 5 intermediate nodes between the levels 3 and 4 (not shown in Figure 4 to avoid confusion) which we denote as “ $C_1^4, C_i^3$ ”; where  $i = 1, \dots, 5$ . We assign to each of the “ $C_1^4, C_i^3$ ” nodes two states  $\{Healthy, Sat.i\ fault\}$ . Finally, we assign to the formation component ( $C_1^4$ ) two health states:  $X_1^4 = \{Healthy, Faulty\}$ . Since the health states of the nodes “ $C_1^4, C_i^3$ ” and  $C_1^4$  are binary, we have implemented a noisy-OR model (as mentioned in Section 2) above level 3. In the nodes with  $pa(C_p^l) \neq \emptyset$ , we specify CPTs by following our proposed procedure in Section 2. In the subsequent discussion, we demonstrate how CPTs in the ACS nodes in Figure 4 are specified by using our proposed procedure. Since we are considering identical satellites, we constructed a single confusion matrix for the 15 RWs ( $C_1^1, \dots, C_{15}^1$ ). Therefore, in this case, the CPTs that are specified in each of the 5 ACS nodes  $C_i^2$  ( $i = 1, 3, 5, 7, 9$ ) are the same. For demonstration purposes, we consider the

ACS of only Sat-1, i.e., the node  $C_1^2$  in the subsequent discussion.

Specification of the CPTs: To specify the CPT of the node  $C_1^2$ , first note that the parent nodes are three RWs; i.e.,  $pa(C_1^2) = \{C_1^1, C_2^1, C_3^1\}$ . Therefore the number of parent nodes is  $N = 3$ . Consequently, possible number of health states of  $C_1^2$  is  $N + 1 = 4$ , which are given by  $X_1^2 = \{x_0, x_1, x_2, x_3\} = \{Healthy, C_1^1\ fault, C_2^1\ fault, C_3^1\ fault\}$ . The possible number of health states of the parent nodes are  $(m_1 + 1) = (m_2 + 1) = (m_3 + 1) = 3$ . The possible states of each of the parent nodes, as mentioned above, are  $X_i^1 = \{x_0, x_1, x_2\} = \{H, f_f, f_c\}$ ; where  $i = 1, 2, 3$ ,  $H$  represents “Healthy”,  $f_f$  represents a “friction fault”, and  $f_c$  represents a “current fault”. The total number of distributions that are required to be specified is  $\prod_{n=1}^N (m_n + 1) = 27$ . Now, we need to identify the  $N_\lambda + 1$  initial distributions over  $X_1^2$ , where  $N_\lambda = \sum_{j=1}^N m_j = 6$ . The  $N_\lambda + 1 = 7$  initial distributions over  $X_1^2$  are given as follows

- $P(X_1^2 | X_1^1 = x_0, X_2^1 = x_0, X_3^1 = x_0)$
- $P(X_1^2 | X_1^1 = x_1, X_2^1 = x_0, X_3^1 = x_0)$
- $P(X_1^2 | X_1^1 = x_2, X_2^1 = x_0, X_3^1 = x_0)$
- $P(X_1^2 | X_1^1 = x_0, X_2^1 = x_1, X_3^1 = x_0)$
- $P(X_1^2 | X_1^1 = x_0, X_2^1 = x_2, X_3^1 = x_0)$
- $P(X_1^2 | X_1^1 = x_0, X_2^1 = x_0, X_3^1 = x_1)$
- $P(X_1^2 | X_1^1 = x_0, X_2^1 = x_0, X_3^1 = x_2)$

Note that the initial distribution (a) above corresponds to the distribution in (2) and the remaining distributions correspond to the distributions in (1). To specify distribution (a) above, we need to compute the following conditional probabilities:

- $P(X_1^2 = x_0 | X_1^1 = x_0, X_2^1 = x_0, X_3^1 = x_0)$
- $P(X_1^2 = x_1 | X_1^1 = x_0, X_2^1 = x_0, X_3^1 = x_0)$
- $P(X_1^2 = x_2 | X_1^1 = x_0, X_2^1 = x_0, X_3^1 = x_0)$
- $P(X_1^2 = x_3 | X_1^1 = x_0, X_2^1 = x_0, X_3^1 = x_0)$

Note that we have employed fuzzy rule-based component fault diagnosis (refer to Section 2.3) in the fol-

lowing nodes of Figure 4: the 15 RWs ( $C_1^1, \dots, C_{15}^1$ ), the five EPSs ( $C_2^2, C_4^2, C_6^2, C_8^2, C_{10}^2$ ), and the formation component ( $C_4^4$ ). For computing the conditional probability (a.1), we refer to Eq. (9). Since the confusion matrices that are associated with the three parent nodes  $C_1^1$ ,  $C_2^1$ , and  $C_3^1$  are the same, the corresponding belief adjustment factors are the same. In addition, since we do not have any diagnosis algorithm deployed in  $C_1^2$ , the information (the values  $a_{x_n}^2$ ;  $n = 0, 1, 2, 3$ ; refer to the policy that is related to the belief adjustment factor as mentioned in Section 2.2) necessary to determine the belief adjustment factor is not available. However, in this case, we have  $a_{x_i}^1$ ;  $i = 0, 1, 2$ . We assume  $a_{x_n}^2 = 0.95$ ; for  $n = 0, 1, 2, 3$  (close to 1 as mentioned in Section 2.2), and from the “one-versus-all” decision matrices that are obtained from the confusion matrix we have,  $a_{x_0}^1 = 0.937$ ,  $a_{x_1}^1 = 0.893$ , and  $a_{x_2}^1 = 0.941$ . Consequently, we have  $h_{1,0}^{1,0} = h_{2,0}^{1,0} = h_{3,0}^{1,0} = 0.937/0.95 = 0.986$ ,  $h_{1,1}^{1,1} = h_{2,1}^{1,2} = h_{3,1}^{1,3} = 0.893/0.95 = 0.940$ , and  $h_{1,2}^{1,1} = h_{2,2}^{1,2} = h_{3,2}^{1,3} = 0.941/0.95 = 0.991$ . Since all the parent nodes are associated with same confusion matrix, as mentioned above, from the confusion matrix we have,  $P(X_1^1 = \bar{x}_0 | I_1^1 = x_0) = P(X_2^1 = \bar{x}_0 | I_2^1 = x_0) = P(X_3^1 = \bar{x}_0 | I_3^1 = x_0) = 0.071$ . With these values, the conditional probability (a.1) is computed as follows (refer to Eq. (9)):

$$\begin{aligned} P(X_1^2 = x_0 | X_1^1 = x_0, X_2^1 = x_0, X_3^1 = x_0) \\ = 1 - \{(1 - h_{1,0}^{1,0})P(X_1^1 = \bar{x}_0 | I_1^1 = x_0) \\ (1 - h_{2,0}^{1,0})P(X_2^1 = \bar{x}_0 | I_2^1 = x_0) \\ (1 - h_{3,0}^{1,0})P(X_3^1 = \bar{x}_0 | I_3^1 = x_0)\} = 0.999 \end{aligned}$$

For computing the conditional probabilities (a.2), (a.3), and (a.4) we use the above results in Eq. (10) (detail computation is not shown here), and finally obtain the initial distribution (a) as  $P(X_1^2 | X_1^1 = x_0, X_2^1 = x_0, X_3^1 = x_0) = (0.999, 0.0003, 0.0003, 0.0003)$ . Next, to specify the distribution (b), we need to compute the following probabilities

$$\begin{aligned} (b.1) P(X_1^2 = x_0 | X_1^1 = x_1, X_2^1 = x_0, X_3^1 = x_0) \\ (b.2) P(X_1^2 = x_1 | X_1^1 = x_1, X_2^1 = x_0, X_3^1 = x_0) \\ (b.3) P(X_1^2 = x_2 | X_1^1 = x_1, X_2^1 = x_0, X_3^1 = x_0) \\ (b.4) P(X_1^2 = x_3 | X_1^1 = x_1, X_2^1 = x_0, X_3^1 = x_0) \end{aligned}$$

For computing the conditional probability (b.2), we refer to Eq. (6). The value  $P(X_1^1 = x_1 | I_1^1 = x_1) = 0.644$  is obtained from the confusion matrix. Using the value of the belief adjustment factor that was computed earlier as  $h_{1,1}^{1,1} = 0.940$ , the conditional probability is obtained as follows:

$$\begin{aligned} P(X_1^2 = x_1 | X_1^1 = x_1) \\ = h_{1,1}^{1,1} \left( P(X_1^1 = x_1 | I_1^1 = x_1) \right. \\ \left. + P(X_1^1 = x_2 | I_1^1 = x_1) \right) = 0.877 \end{aligned}$$

For computing (b.1), we refer to Eq. (7) and use the conditional probabilities that are available from the confusion matrix according to the following computations

$$\begin{aligned} P(X_1^2 = x_0 | X_1^1 = x_1) \\ = P(X_1^1 = x_0 | I_1^1 = x_1) \prod_{j=2}^3 P(X_j^2 = x_0 | I_j^1 = x_0) \\ = (1 - h_{1,1}^{1,1})P(X_1^1 = x_0 | I_1^1 = x_1) \\ h_{2,0}^{1,0}P(X_2^1 = x_0 | I_2^1 = x_0) \\ h_{3,0}^{1,0}P(X_3^1 = x_0 | I_3^1 = x_0) = 0.003 \end{aligned}$$

For computing (b.3) and (b.4), we use the above results in Eq. (8) (detail computation is not shown here), and finally obtain the initial distribution (b) as  $P(X_1^2 | X_1^1 = x_1, X_2^1 = x_0, X_3^1 = x_0) = (0.003, 0.877, 0.060, 0.060)$ . By following the same procedure, the remaining initial distributions are computed.

The remaining distributions in the CPT are generated by using (12). As an example, the distribution associated with two different faults (a “friction fault” in the RW-1 and a “current fault” in the RW-3) is computed by assigning weights (this should be assigned by the human expert) as follows:

$$P(X_1^2 | X_1^1 = x_1, X_2^1 = x_0, X_3^1 = x_2) = w_2(b) + w_7(g) = (0.0015, 0.4407, 0.0323, 0.5255)$$

where  $w_2 = 0.5$  and  $w_7 = 0.5$  (the two faults are believed to be equally possible), and the remaining weights are set to zero. The computation of the distribution (g) and that of other distributions are quite similar, and are not shown here.

#### Node Health State Identification and Evidence

**Generation:** In order to generate the health state evidences that are to be introduced at different nodes of our CDM, we have performed a fuzzy rule-based component fault diagnosis (refer to Section 2.3) for the following components of Figure 4. Specifically, we have the 15 RWs ( $C_1^1, \dots, C_{15}^1$ ), the five EPSs ( $C_2^2, C_4^2, C_6^2, C_8^2, C_{10}^2$ ), and the formation component ( $C_4^4$ ). Note that the health state evidences corresponding to the formation component are introduced at the intermediate nodes (as indicated earlier). Here, as an example, in the case of fault diagnosis of the formation component ( $C_4^4$ ), we depict the Sat-3 rule activation when the above-mentioned friction fault was injected in the Z-axis reaction wheel (subsystem component level) between  $t = 7500$  sec and  $t = 9480$  sec.

Figure 5 shows rule activations in the intermediate node “ $C_1^4, C_3^3$ ” as mentioned above where  $\mu(C_1^4, C_3^3)$  and  $\mu(H)$  represent the rule activations corresponding to a faulty and a healthy condition of Sat-3, respectively. Given the rule activations as shown in Figure 5, an evidence  $e = \{0, 1\}$  (which may be introduced in the intermediate node as described above) is generated whenever rule activation  $\mu(C_1^4, C_3^3) > \mu(H)$ .

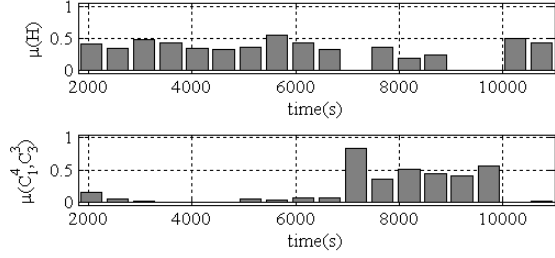


Figure 5: Sat-3 rule activations (the width of each bar-graph is 512 seconds).

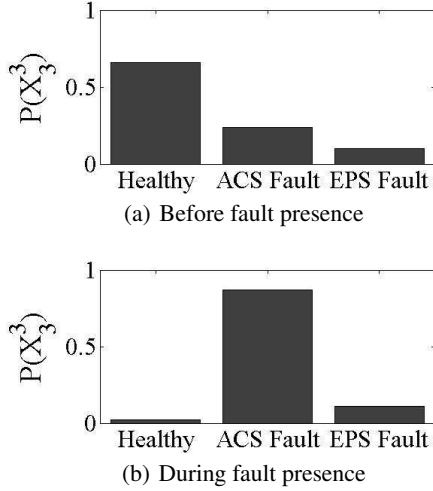


Figure 6:  $P(X_3^3)$  of Sat-3 when an evidence of a fault is introduced at the subsystem component level.

**Hierarchical Diagnosis:** Let us now present certain typical hierarchical fault diagnosis results that are obtained by using our CDM. First, we introduce the fault evidence  $e_9^1 = \{0, 1, 0\}$  (friction fault at Sat-3 RW-Z). Figure 6 shows the probability distributions over the health states of Sat-3 under the fault free condition as well as under the injected friction fault at Sat-3 RW-Z. The distributions clearly justify the existence of a fault in the ACS.

Next, we introduce the fault evidence  $e_{10}^2 = \{0, 0, 1\}$  (battery fault at Sat-5 EPS). Figure 7 shows the probability distributions over the health states of Sat-5 under the injected battery fault at Sat-5 EPS. The distributions clearly justify the existence of a fault in the EPS. The corresponding probability distributions under the fault free conditions are the same as those shown in Figure 6(a).

Finally, we introduce the fault evidence  $\{0, 1\}$  at the intermediate node " $C_1^4, C_3^3$ " (between levels 3 and 4 as discussed before). As stated above, the health state evidences corresponding to the formation components are introduced at the intermediate nodes. The rule activations that are used to generate evidences corresponding to the formation level are shown in Figure 5. Figure 8 shows the probability distributions over the health states of Sat-3 which indicates high probabili-

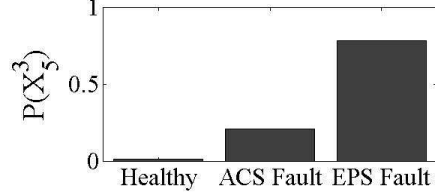


Figure 7:  $P(X_5^3)$  of Sat-5 when an evidence of a fault is introduced at the subsystem level.

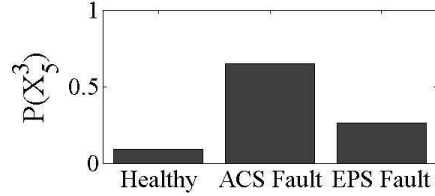


Figure 8:  $P(X_3^3)$  of Sat-3 when an evidence of a fault is introduced at formation level.

ties of ACS and EPS faults in Sat-3 in the presence of the fault evidence at higher (formation) level. Note that in this case the probability of the EPS fault is slightly lower because it was made implicit in the CDM parameters that the ACS is more prone to faults. The corresponding probability distributions under the fault free conditions are the same as those shown in Figure 6(a).

#### 4 MODEL ACCURACY AND VALIDATION

Like any large Bayesian network model, building a BN-based hierarchical fault diagnosis model as we have proposed in this paper involves a careful trade-off between a rich hand-crafted model versus generic dependency model. The design considerations are model parameter and result accuracies, the costs of construction (including the demand for human experts' time), maintenance (including the cost of model updating), and the complexity of probabilistic inference. Consequently, in practice, building such model requires multiple iterations over these tasks until a satisfactory model is achieved.

Our proposed component dependency model (CDM) is a generic model that can be used to decompose complex systems hierarchically in order to perform coherent fault diagnosis. Since the initial distributions are obtained from node fault diagnosis performance data and known health state dependencies, the effort required to develop our proposed model is considerably low in terms of the demand for human experts' time. Furthermore, our model parameters are easy to update when node performance matrix changes due to the availability of new data and improved versions of the node fault diagnosis algorithm. In this case, the initial distributions can be re-computed by following our proposed well-defined procedure, and the weights, if necessary, may be updated.

The main limitation of our proposed method is that the faults that originate in a component at a particular

level are implicitly assumed to be non-interfering with the diagnostic signals of other components (that have a common child node) at the same level. This assumption is reasonable when the fault diagnosis algorithms that are deployed in those nodes are designed to identify faults with a severity range that is low enough not to affect the performances of the other nodes in the same level. Consequently, their influences on the child nodes are to be considered as independent. Note that this limitation arises from the type of information that is made available to our model development. Specifically, according to our problem in hand, the node fault diagnosis algorithms are developed in isolation, and are often proprietary to the design/development teams. Nevertheless, one should investigate the validity of the independence assumptions by using design information and experimental data.

As an example, to investigate the validity of the follower satellites' independence assumptions that are made in Section 2, one can compute the rule activations in one follower satellite in the presence of a fault in another follower satellite. For example, the rule activations corresponding to a healthy satellite Sat-4 is computed in the presence of the previously specified friction fault in the Sat-3's Z-axis reaction wheel. Figure 9 shows the rule activations in the

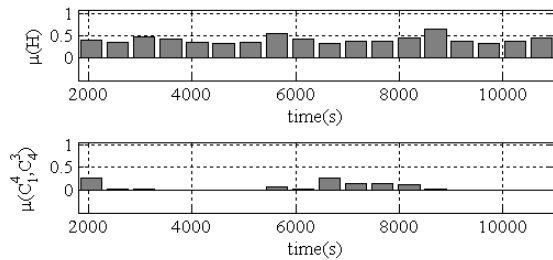


Figure 9: Sat-4 rule activations under the presence of a fault in Sat-3.

intermediate node " $C_1^4, C_4^3$ " as described earlier. It is observed from Figure 9 that the independence assumption is supported by the higher activation level  $\mu(H)$  of the rule corresponding to healthy condition of Sat-4.

**Validation Methods:** It should be noted that in general, diagnosis methods using belief networks is known to be insensitive to imprecision in the probabilities (Henrion *et al.*, 1996) to a large extent. One way to validate our proposed model would be to compare the initial distributions (and hence the CPTs) that are specified by using our proposed procedure with those that are obtained by using the expert beliefs or another method, if available. As an alternative, we are investigating the well-known formal Verification and Validation (V&V) techniques for Bayesian networks such as sensitivity analysis (Bednarskia *et al.*, 2004; Wang, 2006) to validate our proposed model. Biases that are introduced by the prior probabilities and the inaccuracies in conditional probabilities influence the reliability of a BN model's output. Sensitivity analysis is a technique for systematic investigation of the influences of the model inputs and parameters on its

outputs. Since a brute-force method which involves the variation of every single conditional probability, for performing sensitivity analysis is both highly time-consuming and computationally intensive process, our ongoing research is focused on the development of a formal validation procedure for our proposed model. We are investigating how a change in the fault distribution in a confusion matrix would impact the related CPTs which in turn would affect our model output. However, this problem is not within the scope of this paper and is not investigated any further.

## 5 CONCLUSIONS AND FUTURE WORK

In this paper, we have developed a hierarchical fault diagnosis methodology which allows systematic and coherent fault diagnosis in different components or subsystems of a complex formation flight of satellites. The general idea was to decompose a complex system hierarchically into simpler modules or nodes, and perform diagnostic reasoning hierarchically by utilizing the fault diagnosis algorithms that are deployed at different nodes and which are connected via our proposed Bayesian network-based Component Dependency Model (CDM). The model structure was developed from the knowledge of component health state dependencies. A methodology for determining model parameters was developed which demands considerably less effort of the domain experts, and easy to update when node fault diagnosis performances change.

We have demonstrated the effectiveness of our proposed methodology by using synthetic data of a leader-follower formation flight of satellites. The data generation model consists of two subsystems — attitude control subsystem and electrical power subsystem — for each satellite in the formation. We have implemented our proposed CDM by decomposing the formation flying system hierarchically into 4 levels. It is found that when fault evidences were introduced at a node, the states of the remaining nodes of our implemented CDM were updated to reflect the correct health states of the corresponding components. As a part of our ongoing as well as future work, we plan to investigate the validation of our proposed model as well as conduct cost-benefit analysis in a practical environment with real system data.

## ACKNOWLEDGMENTS

This research is supported in part by a Strategic Projects Grant and a Discovery Grant from Natural Sciences and Engineering Research Council of Canada (NSERC).

**NOMENCLATURE**

**List of Symbols**

- $a$  accuracy in fault identification
- $C_p^l$  the  $p$ -th node or component at level  $l$
- $e_p^l$  evidence introduced at  $p$ -th node at level  $l$
- $f_k^l$  the  $k$ -th fault at level  $l$
- $h$  belief adjustment factor
- $I_p^l$  fault identification at node  $C_p^l$
- $L$  maximum number of levels in the hierarchy
- $m_n$  total number of states of the  $n$ -th parent node
- $X_p^l$  the possible health states of  $C_p^l$
- $x_i$  the  $i$ -th health state of a node or component
- $N_\lambda$  total number of initial distributions
- $w$  weight
- $\gamma$  user specified or recommended accuracy

**List of Subscripts**

- 0 non-faulty state
- $i$  state number of a parent node
- $j$  dummy variable
- $k$  fault number, state number, dummy variable
- $K$  maximum value of  $k$
- $m$  node or state number,  
total number of state in a parent node
- $M$  maximum value of  $m$
- $p$  node or component number
- $P$  maximum value of  $p$
- $n$  node or component number,  
state number of a child node
- $N$  maximum value of  $n$

**List of Superscripts**

- $l$  level in the hierarchy
- $n$  state number of a child node
- $p$  node or component number of a child node

**REFERENCES**

- (Barua and Khorasani, 2007) A. Barua and K. Khorasani. Intelligent Model-based Hierarchical Fault Diagnosis for Satellite Formations. In *Proc. 2007 IEEE International Conference on Systems, Man and Cybernetics (SMC 2007)*, Montreal, Canada, October 2007.
- (Barua and Khorasani, 2008) A. Barua and K. Khorasani. Multi-Level Fault Diagnosis in Satellite Formations using Fuzzy Rule-Based Reasoning. In *Proc. 2nd International Symposium on Systems and Control in Aeronautics and Astronautics (ISSCAA 2008)*, Shenzhen, China, December 2008.
- (Barua and Khorasani, 2009) A. Barua and K. Khorasani. Hierarchical Fault Diagnosis and Health Monitoring in Multi-platform Space Systems. In *Proc. 2009 IEEE Aerospace Conference*, Big Sky, Montana, USA, March 2009.
- (Bednarskia *et al.*, 2004) Marcin Bednarskia, Wojciech Cholewa, and Wiktor Frid. Identification of Sensitivities in Bayesian Networks. *Engineering Applications of Artificial Intelligence*, 17:327–335, 2004.
- (Bialke, 1998) B. Bialke. High Fidelity Mathematical Modeling of Reaction Wheel Performance. *Advances in the Astronautical Sciences*, 98:483–496, 1998.
- (Davison and Bird, 2008) Craig R. Davison and Jeff W. Bird. Review of Metrics and Assignment of Confidence Intervals for Health Management of Gas Turbine engines. In *Proc. ASME Turbo Expo 2008*, Berlin, Germany, June 2008.
- (Fenton *et al.*, 2007) N. E. Fenton, M. Neil, and J. G. Caballero. Using Ranked Nodes to Model Qualitative Judgments in Bayesian Networks. *IEEE Transactions on Knowledge and Data Engineering*, 19, No. 10:1420–1432, October 2007.
- (Henrion *et al.*, 1996) Max Henrion, Malcolm Pradhan, Brendan Del Favero, Kurt Huang, Gregory Provan, and Paul O’Rorke. Why is Diagnosis using Belief Networks Insensitive to Imprecision in Probabilities? In *Proc. 12th Annual Conference on Uncertainty in Artificial Intelligence*, pages 307–314, Portland, Oregon, USA, August 1996.
- (Hill, 1878) G. W. Hill. Researches in Luner Theory. *American Journal of Mathematics*, 1, No. 1:5–26, 1878.
- (Iverson, 2008) D. L. Iverson. System Health Monitoring for Space Mission Operations. In *Proc. 2008 IEEE Aerospace Conference*, pages 1–8, Big Sky, Montana, USA, March 2008.
- (Jensen and Nielsen, 2007) F. V. Jensen and T. D. Nielsen. *Bayesian Networks and Decision Graphs*. Springer, NY, USA, 2 edition, 2007.
- (Jiang *et al.*, 2003a) Z. Jiang, R. A. Dougal, and S. Liu. Application of VTB in Design and Testing of Satellite Electrical Power Systems. *Journal of Power Sources*, 122:95–108, 2003.
- (Jiang *et al.*, 2003b) Z. Jiang, S. Liu, and R. A. Dougal. Design and Testing of Spacecraft Power Systems Using VTB. *IEEE Transactions on Aerospace and Electronic Systems*, 39, No. 3:976–989, July 2003.
- (Kahneman *et al.*, 1982) Daniel Kahneman, Paul Slovic, and Amos Tversky. Judgment Under Uncertainty: Heuristics and Biases. In Daniel Kahneman, Paul Slovic, and Amos Tversky, editors, *Judgment Under Uncertainty: Heuristics and Biases*, pages 3–20. Cambridge University Press, Cambridge, 1982.
- (Kurien and R-Moreno, 2008) J. Kurien and M. D. R-Moreno. Cost and Benefits of Model-based Diagnosis. In *Proc. 2008 IEEE Aerospace Conference*, pages 1–14, Big Sky, Montana, USA, March 2008.
- (Laskey and Mahoney, 2000) K. B. Laskey and S. M. Mahoney. Network Engineering for Agile Belief Network Models. *IEEE Transactions on Knowledge and Data Engineering*, 12, No. 4:487–498, July/August 2000.
- (Nikovski, 2000) Daniel Nikovski. Constructing Bayesian Networks for Medical Diagnosis from Incomplete and Partially Correct Statistics. *IEEE Transactions on Knowledge and Data Engineering*, 12, No. 4:509–516, July/August 2000.

- (Pearl, 1988) Judea Pearl. *Probabilistic Reasoning in Intelligent Systems: Networks of Plausible Inference*. Morgan Kaufmann, San Mateo, CA, USA, 1988.
- (Renooij, 2000) Silja Renooij. Probability Elicitation for Belief Networks: Issues to Consider. *The Knowledge Engineering Review*, 163, No. 3:255–269, 2000.
- (SAE, 2008) Health and Usage Monitoring Metrics, Monitoring the Monitor. Society of Automotive Engineers (SAE) Standard, Issuing Committee: E-32 Aerospace Propulsion Systems Health Management, February 2008. Document No. ARP 5783.
- (UCLA, 2009) Automated Reasoning Group UCLA. SAMIAM, Cited: July 2009. <http://reasoning.cs.ucla.edu/samiam/>.
- (USC-VTB-Team, 2009) USC-VTB-Team. Satellite Electrical Power System. USC Virtual Test Bed Homepage, Cited: June 2009. <http://vtb.ee.sc.edu/applications/>.
- (Vadali *et al.*, 2002) S. R. Vadali, S. S. Vaddi, and K. T. Alfriend. An Intelligent Control Concept for Formation Flying Satellites. *International Journal of Robust and Nonlinear Control*, 12:97–115, 2002.
- (Wang, 2006) Haiqin Wang. Using Sensitivity Analysis to Validate Bayesian Networks for Airplane Subsystem Diagnosis. In *Proc. 2006 IEEE Aerospace Conference*, Big Sky, MT, USA, March 2006.